UNSEGMENTED vs. SEGMENTED 4-VANE RFQ: THEORY AND COLD MODEL EXPERIMENTS

A.C. France, O. Delferrière, M. Desmons, Y. Le Noa, G. Novo, O. Piquet
CEA, IRFU, F-91191 Gif-sur-Yvette, France.

Abstract

The RF design of a RFQ should satisfy several conditions, namely: voltage profile required by beam dynamics, a tunable structure, RF stability and reasonable sensitivity to possible perturbations induced by power operation. RF stability requires sufficient separation between accelerating quadrupole mode and adjacent quadrupole and dipole modes. Quadrupole modes separation is directly related to RFQ length, and can be increased if necessary via segmentation; position of dipole modes spectrum with respect to quadrupole spectrum may be adjusted using rod stabilizers inserted at RFQ ends and on either side of coupling circuits. We present a thorough comparison of a single-segment (RFQ_1) vs. a 3-segment (RFQ_3), 6-meter long structure at 352 MHz. Both have been assembled using the modular IPHI cold model, and tuned.

RFQ MODEL

4-Wire Transmission Line Model (TLM)

Both structures are studied with computationally efficient TLM. Field maps in the axial region of a 4-vane RFQ may be approximated by transverse electric-magnetic (TEM) field maps, since there the axial component of magnetic field is close to zero. These TEM field maps are assumed to be supported by a 4-wire system, whose voltage 3-vector U verifies

$$\frac{\partial}{\partial z}\left(C_Q \frac{\partial U}{\partial z}\right) + \frac{1}{c^2} L_Q U = \frac{\omega^2}{c^2} C_Q U, \qquad (1)$$

where z is abscissa, C_Q, L_Q are the capacitance (F/m) and inductance (H.m) matrixes, ω is the radian frequency, c is the speed of light. Quadrupole (U_Q) and dipole (U_S,U_T) components of U are related to inter-electrode voltages by $U_Q = (u_1-u_2+u_3-u_4)/4$, $U_S = (u_1-u_3)/2$, $U_T = (u_2-u_4)/2$. Note that (1) is diagonal for a perfectly symmetric RFQ.

Boundary Conditions (BC)

RFQ ends located in z = a,b, and coupling systems (if any) located in z = z_1,z_2,... are respectively represented by arbitrary lossless 3-port and 6-port circuits, i.e.

$$\partial U(a)/\partial z = -s_a U(a), \quad \left|\begin{matrix}\partial U(z_i^-)/\partial z \\ \partial U(z_i^+)/\partial z\end{matrix}\right| = s_i \left|\begin{matrix}U(z_i^-) \\ U(z_i^+)\end{matrix}\right|, \qquad (2)$$
$$\partial U(b)/\partial z = -s_b U(b),$$

where 3×3 end matrixes $s_{a,b}$ and 6×6 coupling matrixes s_i (in V/m/V units) are symmetric. The operator associated to (1)-(2) is linear unbounded and self-adjoint, with linear bounded and compact inverse. Hence it has a pure point spectrum, with an infinite, countable and bounded from below set of real eigen-values. Solutions for U, (i.e. problem eigen-functions and eigen-values), are found using centered finite difference scheme and standard eigen-solver when s_a, s_b, s_i are independent of frequency. Dispersive s_a, s_b, s_i however require to solve the characteristic equation for eigen-values.

STABILITY ANALYSIS

Standard perturbation theory shows first-order relation between components of voltage error $\Delta V_{Qn,X}$, X = Q,S,T (Q_n is the accelerating mode, with n = 0 for RFQ_1 and n = 3 for RFQ_3), and capacitance errors ΔC_{QQ}, ΔC_{SQ}, ΔC_{TQ} respectively. Here $C_{QQ} = (C_1 + C_2 + C_3 + C_4)/4$, $C_{SQ} = (C_1-C_3)/2$, $C_{TQ} = (C_4-C_2)/2$, and $C_{1...4}$ are the inter-vane capacitances (similar relations hold for inductances). A Dirac-like perturbation in z_0, $\Delta C_{XQ}(z) = \Delta c_{XQ}\,\delta(z-z_0)$, and the resulting voltage error $\Delta V_{Qn,X}$ are related by

$$\frac{\Delta V_{Qn,X}(z)}{V_{Qn,Q}(z)} = h_{XQ}(z,z_0)\frac{\Delta c_{XQ}}{C(z_0)}, \quad X \in \{Q,S,T\}, \qquad (4)$$

where h_{XQ}'s are infinite series involving eigen-functions and eigen-values. The norms $\|h_{XQ}\| = \sup_{z,z0}|h_{XQ}|$ are used to design optimally stable RFQ's (Figure 1).

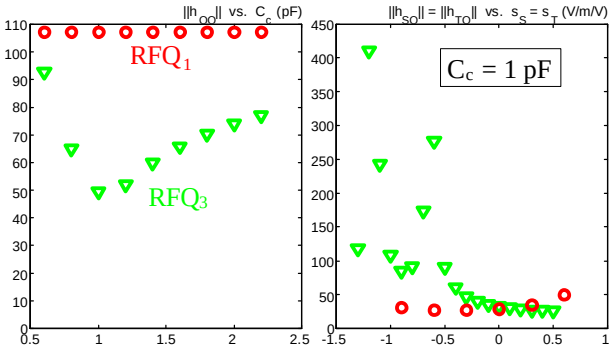

Figure 1: Stability analysis of RFQ_1 and RFQ_3.

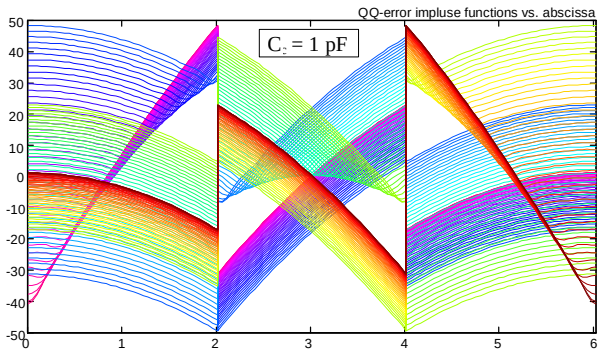

Figure 2: h_{QQ} vs. z (abscissa) and z_0 (color code), RFQ_3.

$\|h_{QQ}\|$ is constant for RFQ_1 but depends on segment coupling capacitance C_c for RFQ_3, whose stability is

improved by a factor ~2 at most for C_c ~1 pF. $\|h_{SQ}\|$, $\|h_{TQ}\|$ depends on diagonal terms $(s_{a,b})_{SS,TT}$; a smooth optimum, identical for RFQ_1 and RFQ_3, is found for $(s_{a,b})_{SS,TT} \sim 0$ (i.e. dipole rods close to quarter-wavelength resonance). An example of h_{XQ} function is given in Figure 2.

RFQ TUNING

Step 1: Dipole Rods Tuning

Lengths of dipole rods are adjusted (with slug tuners in flush position), in order to fit quadratic frequency spacing (QFS) specified by the stability analysis (note that QFS will be only slightly changed by slug tuning). Data in Table 1 was obtained with 152-155 mm (RFQ_1) and 152-152-152-152-155-155 mm (RFQ_3) rods lengths. In both cases, adjacent dipole mode frequencies are slightly higher than desired. Ideal tuning would have been obtained with rods having a longer adjustment range.

Table 1: Dipole Rods Tuning (all values in MHz).

	TLM			measured		
mode	**F**	**ΔF**	**QFS**	**F**	**ΔF**	**QFS**
RFQ_1:						
$\mathbf{D_3}$	345.78	–5.06	–59.31	345.38	–3.19	–47.03
$\mathbf{Q_0}$	350.84	0	0	348.56	0	0
$\mathbf{D_4}$	351.64	+0.80	+23.72	351.19	+2.63	+42.87
RFQ_3:						
$\mathbf{D_{1+1+1}}$	344.17	–6.66	–68.03	346.02	–2.92	–45.05
$\mathbf{Q_{0+0+0}}$	350.83	0	0	348.94	0	0
$\mathbf{D_{2-2-2}}$	358.35	+7.72	+73.03	359.56	+10.62	+86.74

Step 2: End And Coupling Systems Tuning

End plates thicknesses are adjusted to achieve zero voltage slope at RFQ ends, i.e. $(s_a)_{QQ} = 0$, $(s_b)_{QQ} = 0$. Coupling plate thicknesses and coupling gaps are adjusted to achieve zero voltage jump and zero voltage slope across tuning systems, i.e. $s_{ei}^{+} = s_{ei}^{-} = 0$ in s_i matrix elements pertinent for quadrupole mode:

$$(s_i)_{Q^-Q^-} = s_{ei}^{-} + s_{ci}, \qquad (s_i)_{Q^+Q^+} = s_{ei}^{+} + s_{ci},$$

$$(s_i)_{Q^+Q^-} = (s_i)_{Q^+Q^-} = -s_{ci} := -\omega^2 C_c / 4c^2 C .$$

Numerical value of each s matrix is derived from 11 linearly independent excitations $(U, \partial U/\partial z)_{1\ldots11}$ obtained with preset positions of tuners located at some distance of corresponding boundary.

Table 2: BC Tuning. Thicknesses (t) and gaps (g) are in mm, s parameters in V/m/V and capacitances (C_c) in pF.

	avg.	std. dev.	
End system #1	$(s_a)_{QQ} = +0.0041$	0.013	$t_a = 10$
Coupling system #1	$s_{e1}^{-} = +0.070$	0.012	$t_1^{-} = 9$
	$C_{c1} = 1.06 \pm 0.2$	×	$g_1 = 3.1$
	$s_{e1}^{+} = +0.160$	0.040	$t_1^{+} = 9$
Coupling system #2	$s_{e2}^{-} = +0.0080$	0.0087	$t_2^{-} = 9$
	$C_{c2} = 0.95 \pm 0.03$	×	$g_1 = 3.1$
	$s_{e2}^{+} = -0.34$	0.013	$t_2^{+} = 9$
End system #2	$(s_b)_{QQ} = -0.022$	0.010	$t_b = 10$

Table 3: Quadrupole Mode Frequencies (in MHz).

	TLM			measured		
mode	**F**	**ΔF**	**QFS**	**F**	**ΔF**	**QFS**
RFQ_1:						
$\mathbf{Q_0}$	350.84	0	0	348.56	0	0
$\mathbf{Q_1}$	351.73	+0.888	+24.97	349.63	+1.063	+27.24
$\mathbf{Q_2}$	354.37	+3.536	+24.97	352.31	+3.750	+25.63
RFQ_3:						
$\mathbf{Q_{0-1-0}}$	348.85	–1.98	–37.22	347.50	–1.44	–31.64
$\mathbf{Q_{0+0+0}}$	350.83	0	0	348.94	0	0
$\mathbf{Q_{1-1-1}}$	354.26	+3.43	+49.18	352.37	+3.43	+49.10

All parameters are correctly tuned (Table 2), to the exception of s_{e2}^{+}. Measurement accuracy of coupling system #2 has been improved by a better choice of excitations. Quadrupole modes QFS (Table 3) fit TLM values reasonably well.

Step 3: Slugs Tuning

Slugs are adjusted in order to achieve required resonance frequency and voltage profile of accelerating mode, via the iterated procedure described in [3]. Resulting data is presented in Figures 3 (RFQ_1) and 4 (RFQ_3). Voltage profiles are reconstructed according to

$$U = \sum_{i=1}^{M} c_{Qi} \begin{vmatrix} V_{Qi} \\ 0 \\ 0 \end{vmatrix} + \sum_{j=1}^{M} c_{Sj} \begin{vmatrix} 0 \\ V_{Sj} \\ 0 \end{vmatrix} + \sum_{k=1}^{M} c_{Tk} \begin{vmatrix} 0 \\ 0 \\ V_{Tk} \end{vmatrix},$$

where V_{Qi}, V_{Sj}, V_{Tk} are normalized basis eigen-functions:

$$\int_a^b V_{Qi}^2 dz = \int_a^b V_{Sj}^2 dz = \int_a^b V_{Tk}^2 dz = 1 .$$

Amplitudes in {Q,S,T} channels are given in dB units, referenced to amplitude of accelerating mode Q_n:

$$\left[c_{Qi,Sj,Tk}\right]_{dB} = 20 \log \left| c_{Qi,Sj,Tk} / c_{Qn} \right| .$$

Both RFQ's are tuned in 5~6 iterations to ~1% voltage accuracy, corresponding to –45 dB peak relative residual in the M=12 tuned Q-channels (–50 in S,T channels). Peak slug tuner corrections predicted for an additional iteration are about 0.7~0.8 mm, leaving room for improved tuning with some more iterations. RFQ_1 requires about 45% more tuner position range than RFQ_3 (24.7 against 17.0 mm). Final tuning (Table 4) of adjacent quadrupole modes is correct. Adjacent dipole modes are still ~1 MHz too high, but do not compromise stability (cf. the smooth optimum range in Figure 1, right).

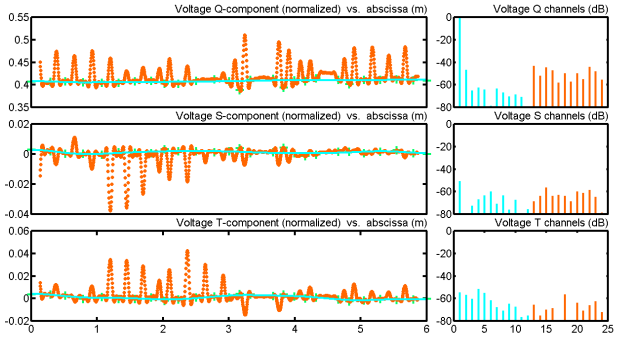

Figure 3: RFQ_1 tuning after last 6th iteration.

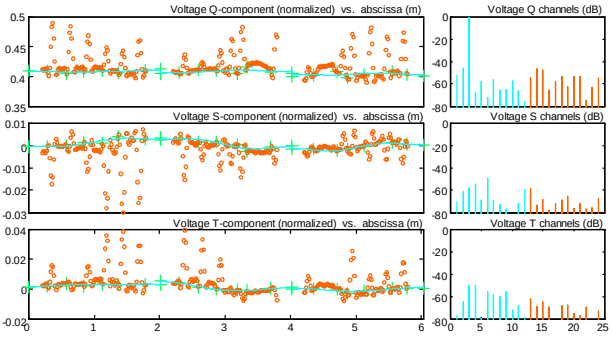

Figure 4: RFQ_3 tuning after last 5th iteration.

Table 4: Frequencies of Adjacent Modes (MHz).

adjacent dipole modes				adjacent quadrupole modes			
mode	**F**	**ΔF**	**QFS**	**mode**	**F**	**ΔF**	**QFS**
RFQ 1:							
D_3	348.25	–3.94	–52.52	**Q_0**	352.19	0	0
Q_0	352.19	0	0	**Q_1**	353.06	+0.874	+24.81
D_4	354.00	+1.81	+35.77	**Q_2**	355.63	+3.437	+24.66
RFQ 3:							
D_{1+1+1}	348.84	–3.38	–48.68	**Q_{0-1-0}**	350.53	–1.69	–34.45
Q_{0+0+0}	352.22	0	0	**Q_{0+0+0}**	352.22	0	0
D_{2-2-2}	361.54	+9.32	+81.56	**Q_{1-1-1}**	355.72	+3.50	+49.79

Step 4: Stability Of Tuned RFQ

Thermal stresses during RFQ operation induce slight geometrical deformations, which in turn induce voltage perturbations. Relative peak voltage error resulting from an arbitrary 10^{-3} relative peak capacitance perturbation is given in Figure 5 for each individual spectral component. Note that alternating the direction of cooling water flow from 1-m section to the next makes geometrical perturbations appear primarily on 6th-order modes (as Q_6 for RFQ_1 or Q_{2+2+2} for RFQ_3), where both RFQ's have similar sensitivities (less than 10^{-2} voltage error for 10^{-3} capacitance error). 6th-order modes are indicated by arrows and boxes in Figure 5.

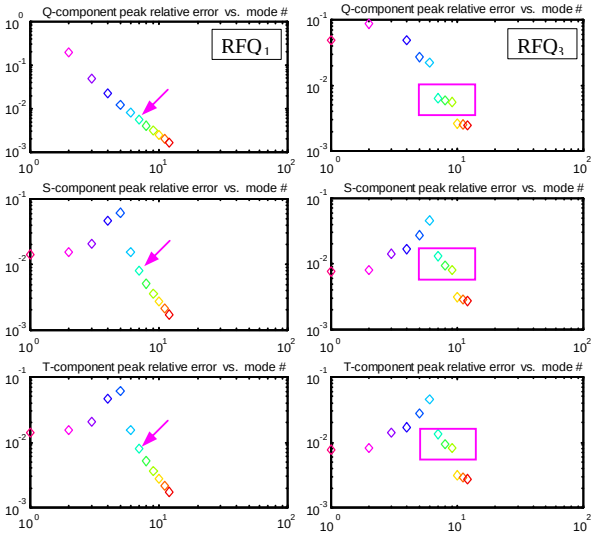

Figure 5: Modal sensitivities.

3D SIMULATIONS

Full-scale 3D simulations of RFQ_1 and RFQ_3, after end and circuit system tuning but prior to slug tuning, have been recently obtained with VectorFields Soprano code [2]. Meshes included 3,382,634 and 4,138,917 elements respectively. Measured and simulated frequencies of adjacent modes are in close agreement (Tables 5 and 6), thus confirming the analysis based on TLM fed with 2D simulations and BC measurements.

Table 5: Adjacent Quadrupole Modes (MHz).

	measured			VectorFields simulation		
mode	**F**	**ΔF**	**QFS**	**F**	**ΔF**	**QFS**
RFQ 1:						
Q_0	348.56	0	0	349.22	0	0
Q_1	349.63	+1.063	+27.24	350.22	+1.002	+26.35
Q_2	352.31	+3.750	+25.63	342.89	+3.672	+25.39
RFQ 3:						
Q_{0-1-0}	347.50	–1.44	–31.64	346.60	–1.58	–31.13
Q_{0+0+0}	348.94	0	0	348.18	0	0
Q_{1-1-1}	352.37	+3.43	+49.10	352.14	+3.96	+52.66

Table 6: Adjacent Dipole Modes (MHz).

	measured			VectorFields simulation		
mode	**F**	**ΔF**	**QFS**	**F**	**ΔF**	**QFS**
RFQ 1:						
D_3	345.37	–3.187	–47.03	345.72	–3.496	–49.29
Q_0	348.56	0	0	349.22	0	0
D_4	351.19	+2.626	+42.87	351.61	+2.386	+40.89
RFQ 3:						
D_{1+1+1}	346.02	–2.92	–45.05	345.48	–2.70	–43.28
Q_{0+0+0}	348.94	0	0	348.18	0	0
D_{2-2-2}	359.56	+10.62	+86.74	358.43	+10.25	+85.10

CONCLUSIONS

Both single-segment and 3-segment, 6-meter long RFQ's turn out to be easily tuned to ~1% voltage accuracy in about 6 iterations; a few more iterations would improve a little bit this accuracy. The single-segment RFQ required ~45% more tuner position range than the 3-segment one. Segmentation reduces overall sensitivity to quadrupole-like perturbations by a factor ~2, but leaves overall sensitivity to dipole-like perturbations unchanged. Stability of RFQ during power operation depends strongly on the spectral contents of perturbations induced by thermal stresses. Alternating the direction of cooling water flow from 1-m section to the next would make geometrical perturbations appear primarily on 6th-order modes, in which case both RFQ's would have similar sensitivities.

REFERENCES

[1] Comsol MultiPhysics commercial software.
[2] VectorFields Soprano commercial software.
[3] O. Piquet, M. Desmons, A. France, "Tuning Procedure Of The 6-Meter IPHI RFQ", EPAC'06, Edinburgh, June 2006, MOPCH107.